

Supernova Studies at ORLaND

A. MEZZACAPPA

Physics Division, Oak Ridge National Laboratory

Bldg. 6010, MS 6354, P.O. Box 2008

Oak Ridge, TN 37831-6354

E-Mail: mezzacappaa@ornl.gov

A new facility to measure neutrino mass differences and mixing angles and neutrino-nucleus cross sections, such as the proposed ORLaND facility at Oak Ridge, would contribute to the experimental determination of vacuum mixing parameters and would provide an experimental foundation for the many neutrino-nucleus weak interaction rates needed in supernova models. This would enable more realistic supernova models and a far greater ability to cull fundamental physics from these models by comparing them with detailed observations. Charged- and neutral-current neutrino interactions on nuclei in the stellar core play a central role in supernova dynamics, nucleosynthesis, and neutrino detection. Measurements of these reactions on select, judiciously chosen targets would provide an invaluable test of the complex theoretical models used to compute the neutrino-nucleus cross sections.

1 Introduction

Core collapse supernovae are among the most energetic explosions in the Universe, releasing 10^{53} erg of energy in the form of neutrinos of all flavors at the staggering rate of 10^{57} neutrinos per second and 10^{45} Watts, disrupting almost entirely stars more massive than 8–10 M_{\odot} and producing and disseminating into the interstellar medium many of the elements in the periodic table. They are a key link in our chain of origins from the Big Bang to the formation of life on Earth; a nexus of nuclear physics, particle physics, fluid dynamics, radiation transport, and general relativity; and serve as laboratories for physics beyond the Standard Model and for matter at extremes of density, temperature, and neutronization that cannot be produced in terrestrial laboratories.

Current supernova theory centers around the idea that the supernova shock wave—formed when the iron core of a massive star collapses gravitationally and rebounds as the core matter exceeds nuclear densities and becomes incompressible—stalls in the iron core as a result of enervating losses to nuclear dissociation and neutrinos. The failure of this “prompt” supernova mechanism sets the stage for a “delayed” mechanism, whereby the shock is reenergized by the intense neutrino flux emerging from the neutrinospheres carrying off the binding energy of the proto-neutron star^{1,2}. The heating is mediated primarily by the absorption of electron neutrinos and antineutrinos on the dissociation-liberated nucleons behind the shock. This process depends critically on the

neutrino luminosities, spectra, and angular distributions, i.e., on the multi-group (multi-neutrino energy) neutrino transport between the proto-neutron star and the shock. This past decade has also seen the emergence of multi-dimensional supernova models, which have investigated the role convection, rotation, and magnetic fields may play in the explosion^{3,4,5,6,7,8,9,10,11,12}.

Realistic supernova models will require extremely accurate neutrino radiation hydrodynamics, but unless advancements in neutrino transport are matched by equally important advancements in nuclear and weak-interaction physics, the efficacy of the former must be called into question. In particular, we must move forward to the use of ensembles of nuclei in the stellar core rather than a single representative nucleus when computing electron and electron neutrino capture during the critical core collapse phase. The use of a single representative nucleus has been the standard until now in virtually all supernova models. Moreover, in computing the electron and electron neutrino capture rates, and in general all of the neutrino–nucleus cross sections, detailed shell model computations must replace the parameterized approximations that have been used in the past. For example, recent work on electron capture up to mass 65 has shown that these parameterized rates can be orders of magnitude in error¹³. The electron capture rate is dominated by Gamow–Teller resonance transitions, with the Gamow–Teller strength distributed over many states. Parameterized treatments place the resonance at a single energy, and this energy is often grossly over- or underestimated relative to the Gamow–Teller centroid computed in realistic shell model computations, leading in turn to rates that are often grossly too small or too large, respectively. (If the centroid is underestimated, more electrons can participate in capture. The reverse is true if the centroid is too high.)

Whereas generations of nuclear structure models will afford ever greater realism in the calculation of stellar core properties and the interactions of core nuclei with the neutrinos flowing through the core, nuclear experiments must be designed and carried out that will serve as guide posts for the theoretical predictions that must be made for the countless rates that enter into any realistic supernova or supernova nucleosynthesis model. In particular, we must have neutrino–nucleus cross section measurements that will help gauge neutrino capture and scattering predictions during stellar core collapse and during the p-, r- and ν -processes after core bounce.

The plan of this paper is as follows. First we give an overview of the state of the art in one- and two-dimensional supernova models, confining our discussion to issues of neutrino transport and convection. For discussions of the role of general relativity, rotation, and magnetic fields in supernova models, the reader may begin with the papers by Bruenn *et al.*¹⁴, Liebendörfer *et al.*^{15,16}, Fryer

and Heger¹¹, Khokhlov *et al.*¹², and MacFadyen and Woosley¹⁷. Our focus will then turn to the nuclear and neutrino science that is input to these models and important for supernova neutrino detection, with an eye toward measurements that could be made at a stopped-pion facility such as ORLAND.

2 One-Dimensional Supernova Models

Although three decades of supernova modeling have established a theoretical framework, fundamental questions about the explosion mechanism remain. Is the neutrino heating sufficient, or are multidimensional effects such as convection and rotation necessary? Can the basic supernova observable, explosion, be reproduced by detailed spherically symmetric models, or are multidimensional models required? In all of their phenomenology, core collapse supernovae are not spherically symmetric. For example, neutron star kicks¹⁸ and the polarization of supernova emitted light¹⁹ cannot arise in spherical symmetry. Nonetheless, ascertaining the explosion mechanism and understanding every explosion observable are two different goals. To achieve both, simulations in one, two, and three dimensions must be coordinated.

The neutrino energy deposition behind the shock depends sensitively on the neutrino luminosities, spectra, and angular distributions in the postshock region. Ten percent variations in any of these quantities can make the difference between explosion and failure in supernova models^{7,20}. Thus, exact multigroup Boltzmann neutrino transport must be considered in supernova models. Past spherically symmetric simulations have implemented increasingly sophisticated approximations to Boltzmann transport: simple leakage schemes²¹, two-fluid models²², and multigroup flux-limited diffusion^{23,24,25}. A generic feature of this last, most sophisticated approximation is that it underestimates the isotropy of the neutrino angular distributions in the heating region and, thus, the heating rate^{26,27}. Failure to produce explosions in the past may have resulted from the use of transport approximations.

To address this question, we model the core collapse, bounce, and post-bounce evolution of a 13 M_{\odot} star, beginning with the precollapse model of Nomoto and Hashimoto²⁸, with a new neutrino radiation hydrodynamics code for both Newtonian and general relativistic spherically symmetric flows: AGILE-BOLTZTRAN. BOLTZTRAN is a three-flavor Boltzmann neutrino transport solver^{29,30}, now extended to fully general relativistic flows¹⁵. In the simulation we include here³¹, it was employed in the $O(v/c)$ limit. AGILE is a conservative general relativistic hydrodynamics code^{15,32}. Its adaptivity enables us to resolve and seamlessly follow the shock through the iron core into the outer stellar layers.

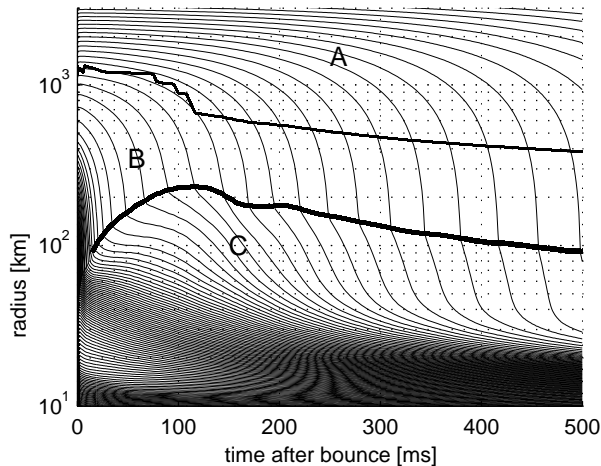


Figure 1: We trace the shock, nuclear burning, and dissociation fronts (the shock and dissociation fronts are coincident), which carve out three regions in the (r, t) plane. A: Silicon. B: Iron produced by infall compression and heating. C: Free nucleons and alpha particles.

Figure 1, taken from the simulation of Mezzacappa *et al.*³¹ shows the radius-versus-time trajectories of equal mass ($0.01M_{\odot}$) shells in the stellar iron core and silicon layer in our Newtonian simulation. Core bounce and the formation and propagation of the initial bounce shock are evident. This shock becomes an accretion shock, decelerating the core material passing through it. At ~ 100 ms after bounce, the accretion shock stalls at a radius ~ 250 km and begins to recede, continuing to do so over the next several hundred milliseconds. No explosion has developed in this model during the first ~ 500 ms.

Thus, we are beginning to answer some fundamental questions in supernova theory. We have shown results from the first ~ 500 ms of our Newtonian core collapse supernova simulation with Boltzmann neutrino transport, initiated from a $13 M_{\odot}$ progenitor. In light of our implementation of Boltzmann transport, if we do not obtain explosions in this model or its general relativistic counterpart when they are completed, or in subsequent models initiated from different progenitors, it would suggest that either changes in our initial conditions (precollapse models) and/or input physics or the inclusion of multidimensional effects such as convection, rotation, and magnetic fields are required ingredients in the recipe for explosion. With the implementation of Boltzmann transport, this conclusion can be made unambiguously. In the past,

it was not clear whether failure or success in supernova models was the result of inadequate transport approximations or the lack of inclusion of important physics.

With regard to improved input physics, the use of ensembles of nuclei in the stellar core rather than a single representative nucleus, computing the neutrino–nucleus cross sections with detailed shell model computations¹³, the inclusion of nucleon correlations in the high-density neutrino opacities^{33,34}, and improvements in precollapse models^{35,36} all have the potential to quantitatively, if not qualitatively, change the details of our simulations. Thus, it is important to note that our conclusions are drawn in the context of the best available input physics.

3 Two-Dimensional Supernova Models: Convection

Supernova convection falls into two categories: (1) convection near or below the neutrinospheres, which we refer to as proto-neutron star convection and (2) convection between the gain radius and the shock, which we refer to as neutrino-driven convection. Proto-neutron star convection may aid the explosion mechanism by boosting the neutrinosphere luminosities, transporting by convection hot, lepton-rich matter to the neutrinospheres. Neutrino-driven convection may aid the explosion mechanism by boosting the shock radius and the neutrino heating efficiency, thereby facilitating shock revival.

3.1 Proto-Neutron Star Convection

This mode of convection may develop owing to instabilities caused by lepton and entropy gradients established by the deleptonization of the proto-neutron star via electron neutrino escape near the electron neutrinosphere and by the weakening supernova shock. (As the shock weakens, it causes a smaller entropy jump in the material flowing through it.) Proto-neutron star convection is arguably the most difficult to investigate numerically because the neutrinos and the matter are coupled, and, consequently, multidimensional simulations must include both multidimensional hydrodynamics and multidimensional, multi-group neutrino transport.

In certain regions of the stellar core, neutrino transport can equilibrate a convecting fluid element with its surroundings in both entropy and lepton number on time scales shorter than convection time scales, rendering the fluid element nonbuoyant. This will occur in intermediate regimes in which neutrino transport is efficient but in which the neutrinos are still strongly enough coupled to the matter. Figures 2 and 3, from Mezzacappa *et al.*⁸, demonstrate that this equilibration can in fact occur. Figure 2 shows the onset and

development of proto-neutron star convection in a $25 M_{\odot}$ model shortly after bounce in a simulation that did not include neutrino transport, i.e., that was a hydrodynamics-only run. Figure 3 on the other hand shows the lack of any significant onset and development of convection when neutrino transport was included in what was otherwise an identical model. Transport’s damping effects are obvious. (The same result occurred in our $15 M_{\odot}$ model.)

On the other hand, in the model of Keil *et al.*³⁷, vigorous proto-neutron star convection developed, which then extended deep into the core as a deleptonization wave moved inward, owing to neutrinos diffusing outward. In this model, convection occurs very deep in the core where neutrino opacities are high and transport becomes inefficient in equilibrating a fluid element with its surroundings.

It is important to note in this context that Mezzacappa *et al.* and Keil *et al.* used complementary transport approximations. In the former case, spherically symmetric transport was used, which maximizes lateral neutrino transport and overestimates the neutrino–matter equilibration rate; in the latter case, ray-by-ray transport was used, which minimizes (zeroes) lateral transport and underestimates the neutrino–matter equilibration rate.

These different outcomes clearly demonstrate that to determine whether or not proto-neutron star convection exists and, if it exists, is vigorous will require simulations coupling three-dimensional, multigroup neutrino transport and three-dimensional hydrodynamics. Moreover, realistic high-density neutrino opacities will be needed.

3.2 Neutrino-Driven Convection

This mode of convection occurs directly between the gain radius and the stalled shock as a result of the entropy gradient that forms as material infalls between the two while being continually heated. In Figure 5, a sequence of two-dimensional plots of entropy are shown, illustrating the development and evolution of neutrino-driven convection in our $15 M_{\odot}$ model⁹. High-entropy, rising plumes and lower-entropy, denser, finger-like downflows are seen. The shock is distorted by this convective activity.

In the Herant *et al.*⁵ simulations, large-scale convection developed beneath the shock, leading to increased neutrino energy deposition, the accumulation of mass and energy in the gain region, and a thermodynamic engine that ensured explosion, although Herant *et al.* stressed the need for more sophisticated multidimensional, multigroup transport in future models. [They used two-dimensional “gray” (neutrino-energy–integrated, as opposed to multigroup) flux-limited diffusion in neutrino-thick regions and a neutrino lightbulb ap-

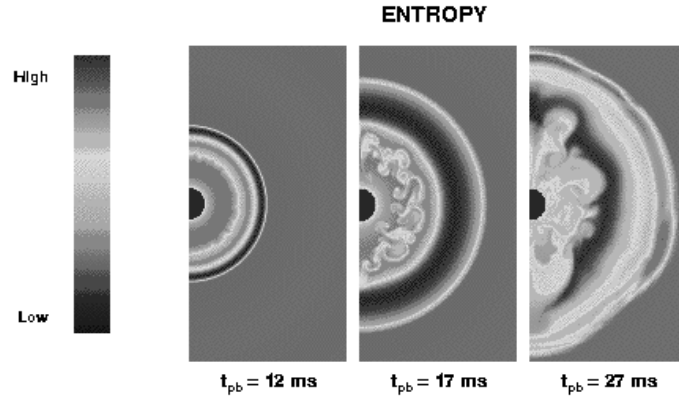


Figure 2: Two-dimensional entropy plots showing the evolution of proto-neutron star convection in our hydrodynamics-only $25 M_{\odot}$ model at 12, 17, and 27 ms after bounce.

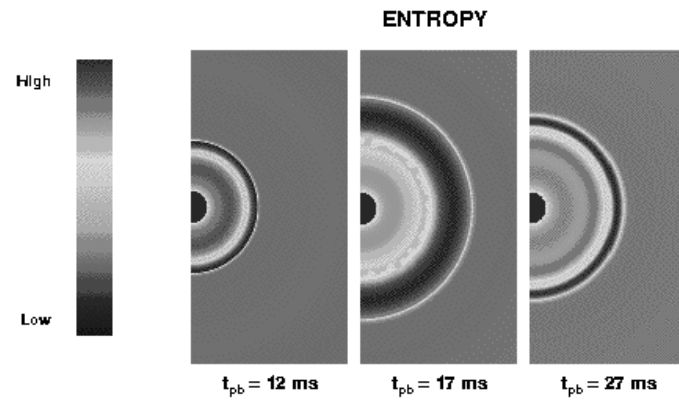


Figure 3: Two-dimensional entropy plots showing the evolution of proto-neutron star convection in our hydrodynamics-plus-neutrino-transport $25 M_{\odot}$ model at 12, 17, and 27 ms after bounce.

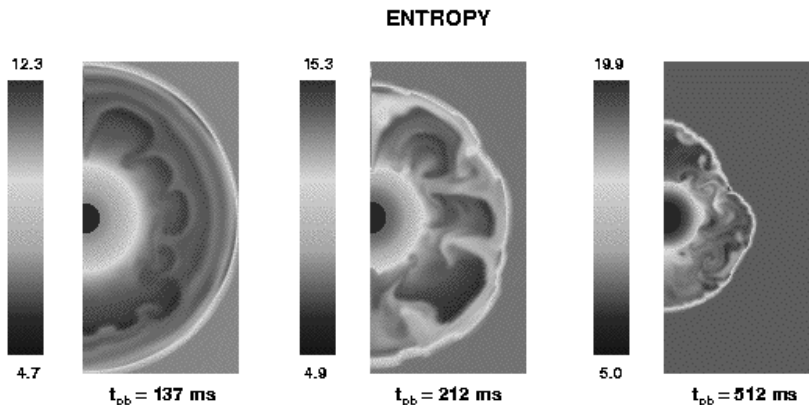


Figure 4: Two-dimensional entropy plots showing the evolution of neutrino-driven convection in our $15 M_{\odot}$ model at 137, 212, and 512 ms after bounce.

proximation in neutrino-thin regions. In a lightbulb approximation, the neutrino luminosities and rms energies are assumed constant with radius.] In the Burrows *et al.* simulations⁶, neutrino-driven convection in some models significantly boosted the shock radius and led to explosions. However, they stressed that success or failure in producing explosions was ultimately determined by the values chosen for the neutrino spectral parameters in their gray ray-by-ray (one-dimensional) neutrino diffusion scheme. (In spherical symmetry (1D), all rays are the same. In a ray-by-ray scheme in axisymmetry (2D), not all rays are the same, although the transport along each ray is a 1D problem. In the latter case, lateral transport between rays is ignored.) Focusing on the neutrino luminosities, Janka and Müller⁷, using a central adjustable neutrino lightbulb, conducted a parameter survey and concluded that neutrino-driven convection aids explosion only in a narrow luminosity window ($\pm 10\%$), below which the luminosities are too low to power explosions and above which neutrino-driven convection is not necessary. In more recent simulations carried out by Swesty¹⁰ using two-dimensional gray flux-limited diffusion in both neutrino-thick and neutrino-thin regions, it was demonstrated that the simulation outcome varied dramatically as the matter–neutrino “decoupling point,” which in turn sets the neutrino spectra in the heating region, was varied within reasonable limits. (The fundamental problem in gray transport schemes is that the neutrino spectra, which are needed for the heating rate, are not computed. The spectra

are specified by choosing a neutrino “temperature,” normally chosen to be the matter temperature at decoupling. In a multigroup scheme, the spectra are by definition computed.) In our two-dimensional models, the angle-averaged shock radii do not differ significantly from the shock trajectories in their one-dimensional counterparts, and no explosions are obtained, as seen in Figure 6. Neither the luminosities nor the neutrino spectra are free parameters. Our two-dimensional simulations implemented spherically symmetric (1D) multigroup flux-limited diffusion neutrino transport, compromising transport dimensionality to implement multigroup transport and a seamless transition between neutrino-thick and neutrino-thin regions.

In light of the neutrino transport approximations made, the fact that all of the simulations have either been one- or two-dimensional, and the mixed outcomes, next-generation simulations will have to reexplore neutrino-driven convection in the context of three-dimensional simulations that implement more realistic multigroup three-dimensional neutrino transport.

4 Neutrino–Nucleus Cross Sections

Neutrino–nucleus cross sections of relevance to supernova astrophysics fall into three categories: cross sections for (1) supernova dynamics, (2) supernova nucleosynthesis, and (3) terrestrial supernova neutrino detection.

4.1 Supernova Dynamics

Whether or not a supernova occurs is set at the time the shock forms and the entire post–stellar-core-bounce evolution is set in motion. Where the shock forms in the stellar core at bounce and how much energy it has initially are set by the “deleptonization” of the core during collapse. The deleptonization occurs as electrons are captured on the free protons and iron-group nuclei in the core, producing electron neutrinos that initially escape. Deleptonization would be complete if electron capture continued without competition, but at densities of order 10^{11-12} g/cm³, the electron neutrinos become “trapped” in the core, and the inverse reactions—charged-current electron neutrino capture on neutrons and iron-group nuclei—begin to compete with electron capture until the reactions are in weak equilibrium and the net deleptonization of the core ceases on a core collapse time scale. The equilibration of electron neutrinos with the stellar core occurs at densities between 10^{12-13} g/cm³. Additionally, as the stellar core densities increase, the characteristic nuclei in the core increase in mass, owing to a competition between Coulomb contributions to the nuclear free energy and nuclear surface tension. For densities of order 10^{13}

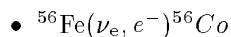
ρ (g/cm ³)	Y_e	T (MeV)	A	Z	$\langle \epsilon_{\nu_e} \rangle$ (MeV)
10 ¹¹	0.4	1	70	30	12
10 ¹²	0.35	2	88	36	19
10 ¹³	0.3	4	138	52	43

g/cm³, the nuclear mass is of order 140. Thus, cross sections for charged-current electron neutrino capture on iron-group nuclei through mass 100 are needed to accurately simulate core deleptonization and to accurately determine the postbounce initial conditions.

Table 1 summarizes the thermodynamic conditions in the core at the three densities discussed above and gives the representative nuclear mass and charge and mean electron neutrino energy. The data were taken from a core collapse simulation carried out by Mezzacappa and Bruenn^{38,39}. Electron neutrino capture would remain important until the neutrinos equilibrate with the matter, which in our simulation would occur when the representative nucleus in the core is between mass 88 and 138.

The size of the inner, unshocked core is proportional to $\langle Y_e \rangle^2$, where $\langle Y_e \rangle$ is the *mean* electron fraction in the inner core. Moreover, the shock loses $\sim 10^{51}$ erg of energy (an explosion energy) for every 0.1 M_\odot it dissociates, which is ~ 10 –20% of the total inner core mass. Thus, an ~ 5 –10% change in the mean electron fraction would have a significant impact on the postbounce evolution. The mean electron fraction at bounce results from many capture reactions during infall (on both protons and nuclei; we focus on nuclei here), and it is clear that accurate electron and electron neutrino capture rates are needed and that theory must be checked against experiment even if only in a few strategic cases.

One goal of the proposed ORLaND facility will be to measure the cross section for electron neutrino charged-current capture on ⁵⁶Fe:



Pioneering measurements of this cross section have been performed by the KARMEN collaboration with an experimental uncertainty $\sim 50\%$. Further measurements are required to achieve an accuracy $\sim 10\%$ to adequately test theoretical models. Moreover, the same proposed technique to measure this cross section can be used to measure the electron neutrino capture cross section on any of the following nuclei, several of which are in the critical nuclear mass range mentioned above: ⁷Li, ⁹Be, ¹¹B, ²⁷Al, ⁴⁰Ca, ⁵¹V, ⁵²Cr, ⁵⁵Mn, ⁵⁹Co, ⁹³Nb, ¹¹⁵In, ¹⁸¹Ta, and ²⁰⁹Bi.

4.2 Supernova Nucleosynthesis

There are several “processes” that define supernova nucleosynthesis: (1) Explosive nucleosynthesis, which occurs as a result of compressional heating by the supernova shock wave as it passes through the stellar layers. (2) Neutrino nucleosynthesis or a “neutrino process,” which occurs due to nuclear transmutations in the stellar layers prior to shock passage. (3) A rapid neutron capture or “r” process, which occurs in the neutrino-driven wind that emanates from the proto-neutron star after the explosion is initiated. The neutrinos both drive the wind and interact with the nuclei in it. Moreover, transmutations produced in (2) are postprocessed in (1). Thus, neutrino–nucleus interactions are central to all three nucleosynthesis processes, although indirectly to process (1).

Neutrino Nucleosynthesis

Neutrino nucleosynthesis is driven by the spallation of protons, neutrons, and alpha particles from nuclei in the stellar layers by the intense neutrino flux that is emanating from the central proto-neutron star powering the supernova⁴⁰. Moreover, neutrino nucleosynthesis continues after the initial inelastic scattering reactions and the formation of their spallation products. The neutrons, protons, and alpha particles released continue the nucleosynthesis through further reactions with other abundant nuclei in the high-temperature supernova environment, generating new rare species. Neutrino nucleosynthesis occurs in two stages: (1) through the neutrino irradiation and nuclear reactions prior to shock arrival and (2) through the continuation of nuclear reactions induced by neutrinos as the stellar layers expand and cool. Neutrino nucleosynthesis is thought to be responsible for the production of, for example, ^{11}B , ^{19}F , and two of Nature’s rarest isotopes: ^{138}La and ^{180}Ta .

The production of the two isotopes, ^{11}B and ^{10}B , appears observationally to be linear with metallicity, i.e., primary mechanisms that operate early in the history of our galaxy produce as much of these isotopes as secondary (quadratic) mechanisms that operate after the Galaxy has been enriched with metals. On the other hand, according to current models, neutrino nucleosynthesis in supernovae, which is a primary process, is not expected to have produced much ^{10}B , unlike the secondary process, cosmic ray spallation. Thus, a laboratory calibration of the spallation channels producing these two isotopes that can be used in conjunction with future HST observations discriminating between ^{10}B and ^{11}B would be invaluable in resolving this controversy and in supporting the theory that neutrino nucleosynthesis in supernovae is an important source of ^{11}B in the Galaxy⁴¹. ^{11}B and ^{10}B are produced through the following spallation channels:

- $^{12}\text{C}(\nu, \nu' \text{p})^{11}\text{B}$
- $^{12}\text{C}(\nu, \nu' \text{n})^{11}\text{C}(e^+, \nu)^{11}\text{B}$
- $^{12}\text{C}(\nu, \nu' \text{d})^{10}\text{B}$
- $^{12}\text{C}(\nu, \nu' \text{pn})^{10}\text{B}$

The final abundance of ^{19}F produced in a supernova can serve as a “supernova thermometer.” If the abundance of ^{19}F produced in the supernova is attributed to neutrino nucleosynthesis, the ratio of $[\text{}^{19}\text{F}/\text{}^{20}\text{Ne}]/[\text{}^{19}\text{F}/\text{}^{20}\text{Ne}]_{\odot}$ (the denominator is the measured ratio in the Sun) is a measure of the muon and tau neutrinosphere temperatures⁴¹. ^{19}F is produced through the following spallation channels⁴¹:

- $^{20}\text{Ne}(\nu, \nu' \text{n})^{20}\text{Ne}^* \rightarrow ^{19}\text{Ne} + \text{n} \rightarrow ^{19}\text{F} + e^+ + \nu_e + \text{n}$
- $^{20}\text{Ne}(\nu, \nu' \text{n})^{20}\text{Ne}^* \rightarrow ^{19}\text{F} + \text{p}$

No obvious site for the production of the rare isotopes, ^{138}La and ^{180}Ta , has been proposed. That they can be produced via neutrino nucleosynthesis in supernovae is compelling, and may be very important in that their existence, however rare, may be a fingerprint of the neutrino process. ^{138}La , and ^{180}Ta are produced through the following spallation channels:

- $^{139}\text{La}(\nu, \nu' \text{n})^{138}\text{La}$
- $^{181}\text{Ta}(\nu, \nu' \text{n})^{180}\text{Ta}$

Experiments to measure the cross sections for all of these spallation channels are being considered as part of a second wave of experiments at ORLaND.

The r-Process

The site for the astrophysical r-process (rapid neutron capture process) is not yet certain, but the leading candidate is the neutrino-driven wind emanating from the proto-neutron star after a core collapse supernova is initiated⁴². The r-process is thought to be responsible for roughly half of the Solar System’s supply of heavy elements. As the neutrino-driven wind expands rapidly and cools, charged particle reactions “freeze out” while neutron capture reactions continue on the “seed” nuclei present at freeze-out. Neutron capture (n, γ) reactions come into equilibrium with neutron disintegration (γ, n) reactions as an equilibrium is established between the free neutrons and the nuclei in the wind. The (n, γ)-(γ, n) equilibrium produces nuclei that are quite neutron rich. Nuclei with half lives short compared to the time scale for the r-process

beta decay, producing nuclei with higher Z and leading to the synthesis of heavier elements. The simultaneous operation of these three types of reactions in the wind and the accompanying nucleosynthesis constitutes the r-process⁴³.

Qian *et al.*⁴⁴ in both the $(n, \gamma) \leftrightarrow (\gamma, n)$ equilibrium and the “postprocessing phase” after these reactions fall out of equilibrium have demonstrated that neutrino-induced reactions can significantly alter the r-process path and its yields. In the presence of a strong neutrino flux, ν_e -induced charged current reactions on the waiting point nuclei at the magic neutron numbers $N = 50, 82, 126$ might compete with beta decays and speed up passage through the bottlenecks there. Also, neutrinos can inelastically scatter on r-process nuclei via ν_e -induced charged-current reactions and ν -induced neutral-current reactions, leaving the nuclei in excited states that subsequently decay via the emission of one or more neutrons. This postprocessing may for example shift the abundance peak at $A = 195$ to smaller mass. Taking things one step further, Haxton *et al.*⁴⁵ pointed out that neutrino postprocessing effects would provide a fingerprint of a supernova r-process. Eight abundances are particularly sensitive to the neutrino postprocessing: ^{124}Sn , ^{125}Te , ^{126}Te , ^{183}W , ^{184}W , ^{185}Re , ^{186}W , and ^{187}Re . *Observed abundances of these elements are consistent with the postprocessing of an r-process abundance pattern in a neutrino fluence consistent with current supernova models.*

On a more pessimistic note, Meyer, McLaughlin, and Fuller⁴⁶ have investigated the impact of neutrino–nucleus interactions on the r-process yields and have discovered that electron neutrino capture on free neutrons and heavy nuclei (in the presence of a strong enough neutrino flux) can actually hinder the r-process by driving the neutrino-driven wind proton rich, posing a severe challenge to theoretical models.

During the r-process and subsequent postprocessing in the supernova neutrino fluence, neutrinos interact with radioactive, neutron-rich nuclei. Thus, relevant direct neutrino–nucleus measurements cannot be made. However, indirect measurements of charged- and neutral-current neutrino–nucleus interactions on stable nuclei that serve to gauge theoretical predictions would be invaluable.

4.3 Supernova Neutrino Detection

The nineteen neutrino events detected by IMB and Kamiokande for SN1987A confirmed the basic supernova paradigm—that core collapse supernovae are neutrino-driven events—and marked the birth of extra-Solar-System neutrino astronomy. For a Galactic supernova, thousands of events will be seen by Super-K and SNO, which, for the first time, will give us detailed neutrino

“lightcurves” and bring us volumes of information about the deepest regions in the explosion. In turn, these lightcurves can be used to test and improve supernova models and their offshoot predictions. Moreover, comparing these detailed neutrino lightcurves with sophisticated supernova models could provide evidence for neutrino oscillations.

Among the neutrino–nucleus interactions of relevance for supernova neutrino detection are neutrino interactions on deuterium in SNO, ^{16}O in Super-K, and ^{56}Fe and $^{206,207,208}\text{Pb}$ in the proposed neutrino detector, OMNIS.

Deuterium: SNO

The four main channels for supernova neutrino detection in SNO are: $\nu + e^- \rightarrow \nu + e^-$, $\nu + d \rightarrow \nu + p + n$, $\nu_e + d \rightarrow p + p + e^-$, and $\bar{\nu}_e + d \rightarrow n + n + e^+$. Measurement of the reaction

- $\nu_e + d \rightarrow p + p + e^-$

at ORLaND, which is being considered to calibrate the reaction $p + p \rightarrow d + e^+ + \nu_e$ (part of the chain of reactions powering the Sun), would also provide a calibration of the SNO neutrino detector. Monte Carlo studies suggest that two years of data in approximately thirty fiducial tons of D_2O would yield a cross section measurement with an accuracy of a few percent⁴⁷, which, in turn, will enable a more accurate interpretation of the SNO data from the next Galactic supernova. The deuterium measurement is among the first wave of planned experiments at ORLaND.

Oxygen: Super-K

The charged-current reaction $^{16}\text{O}(\nu_e, e^-)^{16}\text{F}$ is the principle channel for electron neutrino interactions for thermal sources in the range $T_{\nu_e} \geq 4 - 5$ MeV and its rate exceeds that of neutrino–electron scattering by an order of magnitude for $T_{\nu_e} \geq 7 - 9$ MeV⁴⁸. Moreover, the electron angular distribution is strongly correlated with the electron neutrino energy, providing a way to measure the incident neutrino energy and, consequently, the electron neutrino spectra. By inference, one would then be able to measure, for example, the electron neutrinosphere temperature in a core collapse supernova, i.e., we would have a supernova thermometer⁴⁷. In addition, the appearance of back-angle electron emission from this reaction in, for example, Super-K would result from very energetic electron neutrinos, more energetic than predicted by supernova models. This would be evidence for flavor oscillations⁴⁷. Muon and tau neutrinos in the stellar core couple to the core material only via neutral currents, whereas electron neutrinos and antineutrinos couple via both neutral and charged currents. As a result, the former decouple at higher density and, therefore, temperature, and have harder spectra. *In fact, terrestrial detection*

of the tau and electron neutrinos from a Galactic or near-extra-Galactic core collapse supernova may be our only hope of ever observing oscillations between these two neutrino flavors if the mixing angle is small.

Utilizing reactions on ^{16}O , Langanke, Vogel, and Kolbe⁴⁹ have suggested a novel way of also unambiguously identifying muon and tau neutrino signatures in Super-K. The large average energies for these neutrino flavors are sufficient to excite giant resonances via the neutral-current reactions $^{16}\text{O}(\nu_{\mu,\tau}, \nu'_{\mu,\tau})^{16}\text{O}^*$. These resonances are above particle threshold and subsequently decay via the emission of protons, neutrons, and gamma rays. The gamma rays would provide the muon and tau neutrino signatures. The two decay channels are: $^{16}\text{O}^* \rightarrow ^{15}\text{O} + \text{n} + \gamma$ and $^{16}\text{O}^* \rightarrow ^{15}\text{N} + \text{p} + \gamma$.

Thus, accurate measurements of both charged- and neutral-current neutrino cross sections on ^{16}O would be foundational to interpreting the neutrino data from the next Galactic core collapse supernova and to using that data to potentially observe, for the first time, flavor oscillations involving the tau and electron neutrinos.

An experiment to measure the cross section for:

- $^{16}\text{O}(\nu_e, e^-)^{16}\text{F}$

is among the first proposed experiments at ORLaND. Future experiments may focus on the cross sections for:

- $^{16}\text{O}(\nu_{\mu}, \nu'_{\mu}\text{n}\gamma)^{15}\text{O}$
- $^{16}\text{O}(\nu_{\mu}, \nu'_{\mu}\text{p}\gamma)^{15}\text{N}$

Iron and Lead: OMNIS

The use of iron and lead in OMNIS would provide yet another way of measuring neutrino oscillations in core collapse supernovae⁵⁰. Iron has a sufficiently high threshold for neutron production via charged-current neutrino interactions that such production is negligible, whereas, in lead, neutrons are produced by both charged- and neutral-current interactions. Oscillations between the more energetic muon and tau neutrinos and the electron neutrinos would boost the charged-current event rate while leaving the neutral-current rate roughly unchanged. Thus, the ratio of the event rate in lead to that in iron would serve as an indicator that oscillations had occurred.

To develop OMNIS, experiments to measure the neutrino-iron and neutrino-lead cross sections at ORLaND have been proposed. For iron, the neutral-current reaction:

- $^{56}\text{Fe}(\nu, \nu')^{56}\text{Fe}^* \rightarrow ^{55}\text{Fe} + \text{n}$

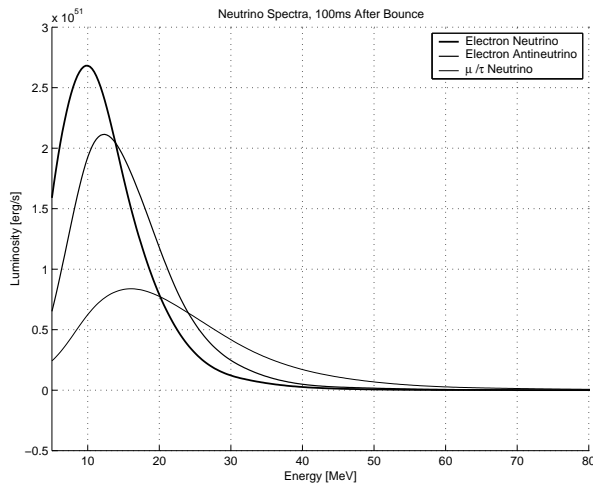


Figure 5: Neutrino spectra from a supernova simulation with Boltzmann neutrino transport initiated from a $13 M_{\odot}$ progenitor. The simulation is fully general relativistic, and the spectra are computed at a radius of 500 km^6 .

dominates. For lead, a total cross section would be measured resulting from the following neutral- and charged-current channels:

- $^{208}\text{Pb}(\nu, \nu')^{208}\text{Pb}^* \rightarrow ^{207}\text{Pb} + \text{n}$
- $^{208}\text{Pb}(\nu, \nu')^{208}\text{Pb}^* \rightarrow ^{206}\text{Pb} + \text{n} + \text{n}$
- $^{208}\text{Pb}(\nu_e, e^-)^{208}\text{Bi}^* \rightarrow ^{207}\text{Bi} + \text{n}$

including the channels for the isotopes ^{206}Pb and ^{207}Pb . The iron and lead cross section measurements are among the first proposed experiments at ORLaND.

5 ORLaND

A new facility to measure neutrino–nucleus cross sections, such as the proposed ORLaND facility at Oak Ridge, would provide an experimental foundation for the many neutrino–nucleus weak interaction rates needed in supernova models. Indeed, we are presented with a unique opportunity, given the intensity of the SNS as a neutrino source and given the overlap (shown in Figures 5 and 6) between the spectra of SNS and supernova neutrinos, to make such measurements. This would enable more realistic supernova models and allow us to cull

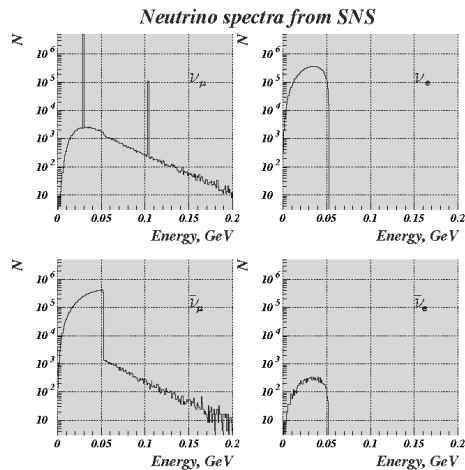


Figure 6: SNS neutrino spectra.

fundamental physics from these models with greater confidence by comparing them with detailed observations. Charged- and neutral-current neutrino interactions on nuclei in the stellar core play a central role in supernova dynamics, nucleosynthesis, and neutrino detection. Measurements of these reactions on select, judiciously chosen targets would provide an invaluable test of the complex theoretical models used to compute the neutrino–nucleus cross sections.

Acknowledgments

A.M. is supported at the Oak Ridge National Laboratory, managed by UT-Battelle, LLC, for the U.S. Department of Energy under contract DE-AC05-00OR22725. AM would like to acknowledge many illuminating discussions with Frank Avignone, John Beacom, Jeff Blackmon, Dick Boyd, David Dean, Yuri Efremenko, Jon Engel, George Fuller, Wick Haxton, Raph Hix, Ken Lande, Karlheinz Langanke, Matthias Liebendörfer, Gabriel Martinez-Pinedo, Gail McLaughlin, Mike Strayer, and Friedel Thielemann, all of which contributed significantly to this manuscript.

References

1. J. R. Wilson. In J. M. Centrella, J. M. LeBlanc, and R. L. Bowers, editors, *Numerical Astrophysics*, page 422, Boston, 1985. Jones and

- Bartlett.
2. H. H. Bethe and J. R. Wilson. *Astrophysical Journal*, 295:14, 1985.
 3. M. Herant, W. Benz, and S. A. Colgate. *Astrophysical Journal*, 395:642, 1992.
 4. D. S. Miller, J. R. Wilson, and R. W. Mayle. *Astrophysical Journal*, 415:278, 1993.
 5. M. Herant, W. Benz, W. R. Hix, C. L. Fryer, and S. A. Colgate. *Astrophysical Journal*, 435:339, 1994.
 6. A. Burrows, J. Hayes, and B. A. Fryxell. *Astrophysical Journal*, 450:830, 1995.
 7. H.-Th. Janka and E. Müller. *Astronomy and Astrophysics*, 306:167, 1996.
 8. A. Mezzacappa, A. C. Calder, S. W. Bruenn, J. M. Blondin, M. W. Guidry, M. R. Strayer, and A. S. Umar. *Astrophysical Journal*, 493:848, 1998.
 9. A. Mezzacappa, A. C. Calder, S. W. Bruenn, J. M. Blondin, M. W. Guidry, M. R. Strayer, and A. S. Umar. *Astrophysical Journal*, 495:911, 1998.
 10. F. D. Swesty. In A. Mezzacappa, editor, *Stellar Explosions, Stellar Evolution, and Galactic Chemical Evolution*, page 539, Bristol, 1998. IoP Publishing.
 11. C. L. Fryer and A. Heger. *astro-ph/9907433*.
 12. A. M. Khokhlov, P. A. Höflich, E. S. Oran, J. C. Wheeler, and A. Yu. Chtchelkanova. *Astrophysical Journal*, 524:L107, 1999.
 13. K.-H. Langanke and G. Martinez-Pinedo. *Nuclear Physics*, A673:481, 2000.
 14. S. W. Bruenn, K. R. DeNisco, and A. Mezzacappa. *Astrophysical Journal*, submitted, 2000.
 15. M. Liebendörfer. PhD thesis, University of Basel, Basel, Switzerland, 2000.
 16. M. Liebendörfer, A. Mezzacappa, F.-K. Thielemann, O. E. B. Messer, W. R. Hix, and S. W. Bruenn. *Physical Review Letters*, submitted, 2000.
 17. A. I. MacFadyen and S. E. Woosley. *Astrophysical Journal*, 524:262, 1999.
 18. C. L. Fryer, A. Burrows, and W. Benz. *Astrophysical Journal*, 496:333, 1998.
 19. J. C. Wheeler. In S. S. Holt, editor, *Cosmic Explosions, A Conference Proceedings*, Melville, 2000. AIP.
 20. A. Burrows and J. Goshy. *Astrophysical Journal Letters*, 416:L75, 1993.

21. K. A. Van Riper and J. M. Lattimer. *Astrophysical Journal*, 249:270, 1981.
22. J. Cooperstein, L. J. Van Den Horn, and E. A. Baron. *Astrophysical Journal*, 309:653, 1986.
23. W. D. Arnett. *Astrophysical Journal*, 218:815, 1977.
24. S. W. Bruenn. In M. W. Guidry and M. R. Strayer, editors, *First Symposium on Nuclear Physics in the Universe*, page 31, Bristol, 1993. IOP Publishing.
25. J. R. Wilson and R. W. Mayle. *Physics Reports*, 227:97, 1993.
26. H.-Th. Janka. *Astronomy and Astrophysics*, 256:452, 1992.
27. O. E. B. Messer, A. Mezzacappa, S. W. Bruenn, and M. W. Guidry. *Astrophysical Journal*, 507:353, 1998.
28. K. Nomoto and M. Hashimoto. *Physics Reports*, 163:13, 1988.
29. A. Mezzacappa and S. W. Bruenn. *Astrophysical Journal*, 405:669, 1993.
30. A. Mezzacappa and O. E. B. Messer. *Journal of Computational and Applied Mathematics*, 109:281, 1998.
31. A. Mezzacappa, M. Liebendörfer, O. E. B. Messer, W. R. Hix, F.-K. Thielemann, and S. W. Bruenn. *Physical Review Letters*, submitted, 2000.
32. M. Liebendörfer and F.-K. Thielemann. In E. Aubourg, T. Montmerle, J. Paul, and P. Peter, editors, *Nineteenth Texas Symposium on Relativistic Astrophysics*, Amsterdam, 2000. Elsevier Science B. V.
33. A. Burrows and R. F. Sawyer. *Physical Review*, C58:554, 1998.
34. S. Reddy, M. Prakash, J. M. Lattimer, and J. A. Pons. *Physical Review*, C59:2888, 1999.
35. G. Bazan and W. D. Arnett. *Astrophysical Journal*, 496:316, 1998.
36. H. Umeda, K. Nomoto, and T. Nakamura. In A. Weiss, editor, *The First Stars*, Berlin, 2000. Springer.
37. W. Keil, H.-Th. Janka, and E. Müller. *Astrophysical Journal Letters*, 473:L111, 1996.
38. A. Mezzacappa and S. W. Bruenn. *Astrophysical Journal*, 405:637, 1993.
39. A. Mezzacappa and S. W. Bruenn. *Astrophysical Journal*, 410:740, 1993.
40. S. E. Woosley, D. H. Hartmann, R. D. Hoffman, and W. C. Haxton. *Astrophysical Journal*, 356:272, 1990.
41. W. Haxton. In *Proceedings of the 1998 TASI Summer School*, 1999.
42. S. E. Woosley, G. J. Mathews, J. R. Wilson, R. D. Hoffman, and B. S. Meyer. *Astrophysical Journal*, 433:229, 1994.
43. B. S. Meyer. *Annual Reviews of Astronomy and Astrophysics*, 32:153, 1994.
44. Y.-Z. Qian, W. C. Haxton, K.-H. Langanke, and P. Vogel. *Physical*

- Review*, C55:1532, 1997.
45. W. C. Haxton, K.-H. Langanke, Y.-Z. Qian, and P. Vogel. *Physical Review Letters*, 78:2694, 1997.
 46. B. S. Meyer, G. C. McLaughlin, and G. M. Fuller. *Physical Review*, C58:3696, 1998.
 47. ORLaND Collaboration. *Workshop on Neutrino-Nucleus Physics Using a Stopped-Pion Facility (ORLaND)*, May 23-26, 2000, Oak Ridge, Tennessee
 48. W. Haxton. *Physical Review*, D36:2283, 1987.
 49. K.-H. Langanke, P. Vogel, and E. Kolbe. *Physical Review Letters*, 76:2629, 1996.
 50. R. N. Boyd. In S. Kubono and T. Kajino, editors, *Origin of Matter and Evolution of Galaxies*, Singapore, 2000. World Scientific.